Journal of Sound and Vibration (2002) **257**(3), 596–604
doi:10.1006/jsvi.2001.4237, available online at http://www.idealibrary.com on IDEAL®

NATURAL FREQUENCIES OF SUSPENSION BRIDGES: AN ARTIFICIAL NEURAL NETWORK APPROACH

M. Çevik

Izmir Vocational School, Dokuz Eylül University, Buca, Izmir, Turkey

AND

E. Özkaya and M. Pakdemirli

Department of Mechanical Engineering, Celal Bayar University, 45140 *Muradiye, Manisa, Turkey*.
E-mail: *mpak@spil.bayar.edu.tr*

1. INTRODUCTION

In the design of suspension bridges, dynamical effects such as wind, traffic, and earthquake play a significant role, so vibrational analysis becomes inevitable. Possible vibrational modes must be determined and corresponding natural frequencies should be calculated as a first step. The natural frequencies of suspension bridges have been calculated by several researchers [1–7]. The free natural vibrational modes of a suspension bridge may be classified as vertical, torsional, and lateral. The real motion of the bridge is a coupled combination of these modes. The most effective, and thus most important, of these modes are vertical and torsional. The equations of coupled vertical and torsional motion have a non-linear form and are very complicated. In order to substitute a basis for non-linear analysis, a preliminary linear analysis is considered in this study. As the vertical and torsional equations have similar forms, by solving the vertical equation, one also obtains the solution of the torsional equation.

When the equation of motion is solved with the given boundary conditions, transcendental equations yielding the natural frequencies are obtained. The equation yielding the frequencies of asymmetric modes has a simple form. In contrast, the equation yielding the frequencies of symmetric modes is very complicated. The natural frequencies of symmetric modes can be found from this equation by using root finding algorithms. In this study, we seek for the relation between the first three natural frequencies and the physical parameters of a suspension bridge; namely, span length, moment of inertia of the bridge cross-section, initial horizontal component of cable tension, dead weight of the bridge per unit length of the span, cables' cross-sectional area, moduli of elasticity of the bridge deck and the cables. The first three natural frequencies are calculated using the Newton–Raphson method for different physical parameters. This technique involving step-by-step numerical iteration for each frequency and group of physical parameters, requires a relatively long computational time. Manual intervention to the program may be needed, since iterations do not converge for all estimated values of the roots. Alternatively, the calculated key values are used in training a multi-layer, feed-forward, back-propagation artificial neural network (ANN) algorithm until the per cent error is below the required value. Then using the trained algorithm, for a given input data set, which can be a huge matrix, natural frequencies are retrieved immediately to within 1·02% error. The ANN

0022-460X/02/$35.00

algorithm does not calculate the frequencies one by one as in the case of the Newton–Raphson algorithm, instead it gives the output in a tabular form without any convergence problems. Finally, the variation of the natural frequencies of the vertical symmetric modes with the above mentioned physical parameters are investigated by using the trained ANN algorithm. The results of the ANN and Newton–Raphson methods are compared and it is found that the ANN modelling can be effectively used as a supplementary technique to conventional numerical procedures in vibration problems. For some other examples of the ANN applications to structural mechanics, the reader is referred to the previous work [8–12].

2. FORMULATION OF THE PROBLEM

The three-span suspension bridge shown in Figure 1 is considered. The non-linear dimensionless equations of motion were derived using Hamilton's principle in reference [13]. The linearized equation of vertical motion is given by

$$\ddot{v}_i + I_s v_i^{\mathrm{iv}} - 2H_w v_i'' + \frac{1}{2}\sum_{j=1}^{3} S_c w_b^2 \int_0^{\ell_j} v_j \,\mathrm{d}x = 0, \tag{1}$$

where v is the vertical displacement of the bridge deck, I_s is the moment of inertia of the bridge cross-section, H_w is the initial horizontal component of cable tension, S_c is a parameter related to the cables' cross-sectional area, virtual length, and moduli of elasticity of the bridge deck and cables; w_b is the dead weight of the bridge per unit length of the span; ℓ_i is the length of the ith span; and i represents ($i = 1, 2, 3$) the number of span. The above parameters are all dimensionless. The dot denotes differentiation with respect to the non-dimensional time t and the prime denotes differentiation with respect to the spatial variable x. The dimensionless quantities are related to the dimensional ones (denoted by asterisks) through the following relations:

$$x = \frac{x^*}{L}, \quad v_i = \frac{v_i^*}{L}, \quad t = \left(\frac{E_s g}{w_b^*}\right)^{1/2} t^*, \quad \ell_i = \frac{\ell_i^*}{L}, \quad I_s = \frac{I_s^*}{L^4},$$

$$H_w = \frac{H_w^*}{E_s L^2}, \quad w_b = \frac{w_b^* L}{H_w^*}, \quad S_c = \frac{E_c A_c}{E_s L_E L}, \quad L_E = \sum_{i=1}^{3} \int_0^{\ell_i} \left(\frac{\mathrm{d}s_i}{\mathrm{d}x_i}\right)^3 \mathrm{d}x_i, \tag{2}$$

where L is a characteristic length used for non-dimensionalization, E_s and I_s are, respectively, the modulus of elasticity and the moment of inertia of the bridge cross-section, g is the gravitational acceleration, E_c and A_c are, respectively, the cables' modulus of ealsticity and the cross-sectional area, L_E is the virtual length (defined in reference [7]). The

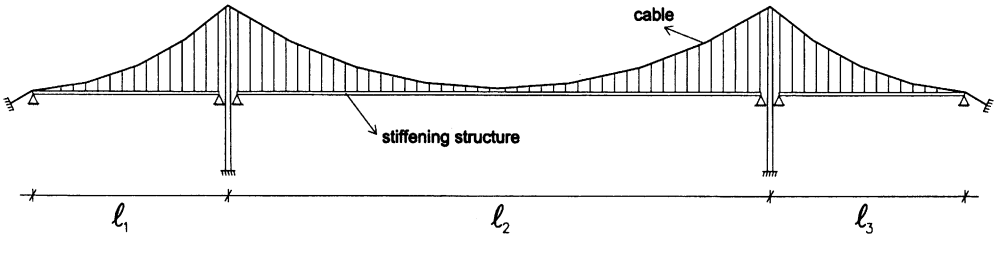

Figure 1. A three-span suspension bridge model.

boundary conditions are:

$$v_i(0,t)=0,\quad v_i(\ell_i,t)=0,\quad v_i''(0,t)=0,\quad v_i''(\ell_i,t)=0. \tag{3}$$

The solution of equation (1) with the boundary conditions (3) can be expressed in the form

$$v_i(x,t)=(A\cos\omega t+B\sin\omega t)\,Y_i(x), \tag{4}$$

where ω is the natural frequency. Substituting equation (4) into equation (1) yields

$$I_sY_i^{iv}-2H_wY_i''+\frac{1}{2}\sum_{j=1}^{3}S_cw_b^2\int_0^{\ell_j}Y_j\,\mathrm{d}x-\omega^2Y_i=0. \tag{5}$$

At this point, there are two independent parts of the problem to be solved separately. For the asymmetric modes, the integral term in equation (5) is zero and the natural frequencies can be calculated with ease. However, for the symmetric modes, since there is an interaction between the center and side spans, the integral term is not zero and the transcendental equation yielding the natural frequencies of symmetric modes is complicated:

$$\sum_{i=1}^{3}\frac{\ell_iw_b^2}{\omega^2(\varphi_i^2+\psi_i^2)}\left(\frac{\varphi_i^2+\psi_i^2}{2}-\frac{\psi_i^2}{\varphi_i}\tan\frac{\varphi_i}{2}-\frac{\varphi_i^2}{\psi_i}\tanh\frac{\psi_i}{2}\right)-\frac{1}{S_c}=0. \tag{6}$$

In this equation

$$\varphi_i=\sqrt{\frac{H_w\ell_i^2}{I_s}\left(\sqrt{1+\frac{I_s\omega^2}{H_w^2}}-1\right)}, \tag{7}$$

$$\psi_i=\sqrt{\frac{H_w\ell_i^2}{I_s}\left(\sqrt{1+\frac{I_s\omega^2}{H_w^2}}+1\right)}. \tag{8}$$

The transcendental equation (6) is solved using the Newton–Raphson procedure for various physical parameters. This is a lengthy process since the algorithm may cause convergence problems. Only the first three natural frequencies are calculated.

3. APPLICATION OF THE ANN ALGORITHM

In this section, an alternative to conventional numerical techniques is presented by employing an ANN algorithm with a multi-layer, feed-forward, back-propagation architecture. The multi-layer perceptron has an input layer, two hidden layers, and an output layer. The input vector representing the pattern to be recognized is incident on the input layer and is distributed to subsequent hidden layers, and finally to the output layer via weighted connections. Each neuron in the network operates by taking the sum of its weighted inputs and passing the result through a non-linear activation function (transfer function). In this study, the sigmoid function is used as the transfer function. The momentum and learning rate values are taken as 0·9 and 0·7, respectively. These values are found by trial and error. A back-propagation algorithm is used in the optimization in which the weights are modified. Although 5000 iterations yield reasonable results, to achieve a satisfactory high precision learning rate, 50 000 iterations have been performed in training the algorithm. The ANN architecture used is a 5 : 12 : 12 : 3 multi-layer architecture as shown in Figure 2.

The problem of finding the frequencies of the system can be treated as an input/output process with an unknown transfer function. There are six-dimensionless parameters in

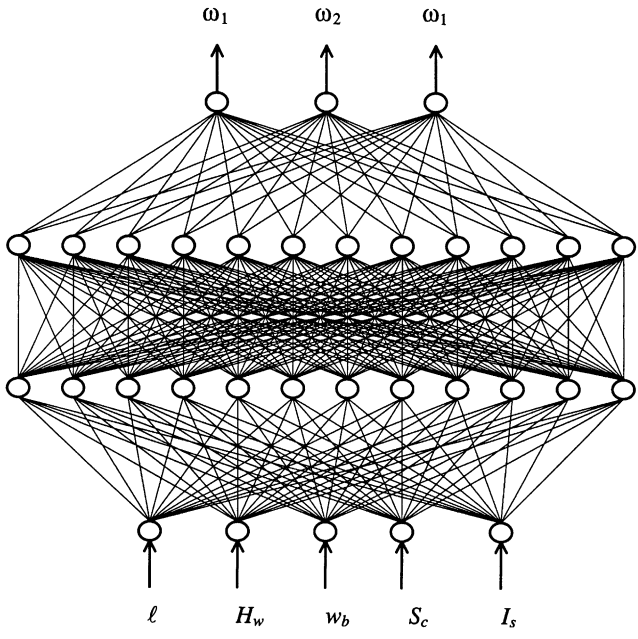

Figure 2. The ANN architecture used in the analysis.

TABLE 1

The values used in input patterns prepared for the training of ANN

ℓ	2·5, 4·2, 5·8, 7·5
H_w	3×10^{-9}, 8×10^{-9}, 15×10^{-9}, 21×10^{-9}, $27{\cdot}5\times10^{-9}$, 39×10^{-9}, 50×10^{-9}
w_b	0·80, 0·64, 0·48, 0·32, 0·22
I_s	6×10^{-10}, 18×10^{-10}, 30×10^{-10}, 40×10^{-10}
S_c	3×10^{-7}, 8×10^{-7}, 14×10^{-7}, 20×10^{-7}

equation (1); namely $\ell_1 = \ell_3$, ℓ_2, H_w, w_b, S_c, and I_s. The ratio of side-to-center spans in three-span bridges is generally $\frac{1}{3}$, so that the length of the side span is approximated to one-third of the center span ($\ell = \ell_2 = 3\ell_1$). Thus, the number of input parameters is reduced to five whereas the corresponding output values are the first three natural frequencies. While preparing input patterns using these values, instead of taking a combination of all values, it is desired to prepare meaningful sets by considering their physical correspondings. In other words, consistent and realistic values are selected. For example, moment of inertia and the cable forces for short span bridges are assumed to have rather low values; whereas, the values are increased depending on the increasing span length. Increasing the input values decreases the error in training; however, preparation and training of the data take a very long time in that case. Considering these criteria, a total of 493 input patterns are prepared. The input values used herein are given in Table 1.

In Figure 3, the mean square errors (MSE) in training versus number of iteration are presented. The MSE dropped drastically after 5000 iterations. Training has been continued up to 50 000 iterations for higher precision, since this task should be done once only. The training phase required an hour or so on a PC with Pentium 350 MHz microprocessor.

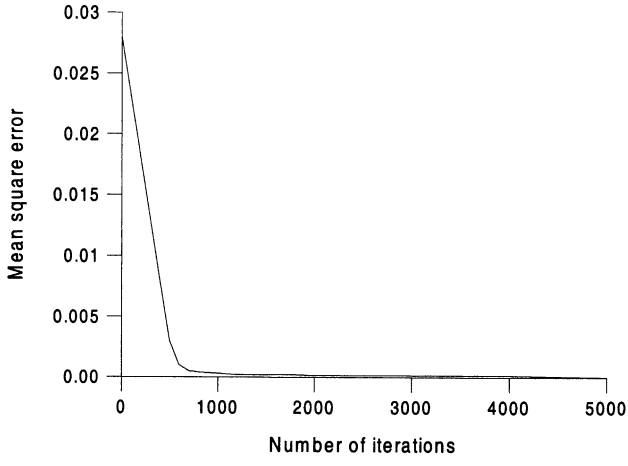

Figure 3. MSE versus number of iterations for training natural frequencies.

TABLE 2

Comparison of the results of the ANN and N–R methods for test values

						Newton–Raphson			ANN		
N	ℓ	H_w	w_b	I_s	S_c	ω_1	ω_2	ω_3	ω_1	ω_2	ω_3
1	3·0	5×10^{-9}	0·60	10×10^{-10}	5×10^{-7}	1·296	2·978	4·315	1·306	2·945	4·401
2	3·8	15×10^{-9}	0·44	20×10^{-10}	15×10^{-7}	1·057	2·667	3·086	1·075	2·664	3·114
3	4·0	20×10^{-9}	0·56	30×10^{-10}	10×10^{-7}	0·888	2·209	2·593	0·906	2·234	2·613
4	4·5	26×10^{-9}	0·50	16×10^{-10}	12×10^{-7}	0·766	1·840	2·191	0·767	1·862	2·199
5	4·8	15×10^{-9}	0·60	34×10^{-10}	10×10^{-7}	0·750	2·021	2·828	0·766	2·022	2·893
6	5·0	20×10^{-9}	0·40	14×10^{-10}	15×10^{-7}	0·779	1·853	2·515	0·776	1·845	2·529
7	5·2	30×10^{-9}	0·30	20×10^{-10}	13×10^{-7}	0·811	1·797	2·109	0·812	1·794	2·080
8	5·5	25×10^{-9}	0·24	16×10^{-10}	18×10^{-7}	0·869	2·003	2·259	0·871	2·000	2·254
9	6·0	$16{\cdot}5\times10^{-9}$	0·30	20×10^{-10}	12×10^{-7}	0·755	1·825	2·380	0·752	1·819	2·376
10	6·2	21×10^{-9}	0·28	40×10^{-10}	10×10^{-7}	0·758	1·847	2·094	0·756	1·835	2·100
11	6·5	$22{\cdot}5\times10^{-9}$	0·24	28×10^{-10}	13×10^{-7}	0·759	1·812	2·087	0·751	1·807	2·085
12	6·8	36×10^{-9}	0·28	10×10^{-10}	15×10^{-7}	0·649	1·453	1·857	0·639	1·449	1·828
13	7·0	33×10^{-9}	0·24	24×10^{-10}	17×10^{-7}	0·692	1·594	1·971	0·681	1·604	1·937
14	7·2	36×10^{-9}	0·32	30×10^{-10}	10×10^{-7}	0·585	1·352	1·689	0·575	1·351	1·700
15	7·4	$32{\cdot}5\times10^{-9}$	0·24	36×10^{-10}	8×10^{-7}	0·636	1·422	1·633	0·630	1·423	1·636

After the training is completed, the results of the ANN and Newton–Raphson (N–R) methods are compared for 15 test patterns. The input and output values for these patterns are shown in Table 2.

In Table 3, average percentage errors for training and test values of ANN are given. In general, a good agreement is observed. For the input values given in Table 1, the ANN algorithm produced results with an average error of less than 0·85%. For the test values given above, results are compared for both methods and it is found that the maximum error is less than 1·02%. These values are shown in Table 3. From an engineering point of view, these errors are considerably low.

It should be noted that the ANN requires a relatively long time in the training phase. Once the training is completed, however, for a given matrix of input values, the output

TABLE 3

Average percentage errors for training and test values of ANN

	ω_1	ω_2	ω_3
Training values (%)	0·849	0·738	0·838
Test values (%)	1·011	0·442	0·878

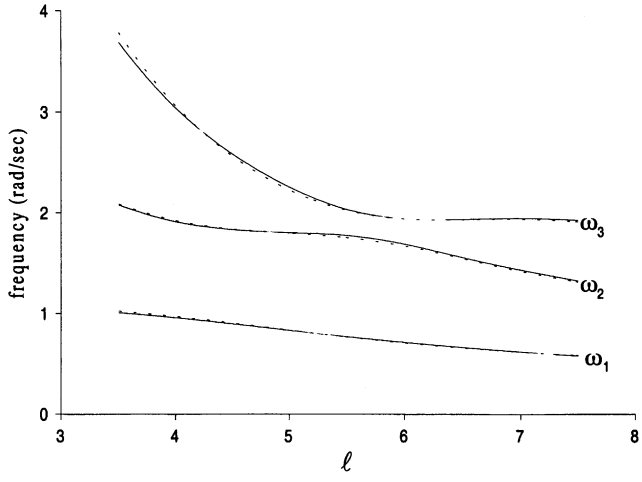

Figure 4. Variation of natural frequency with the dimensionless parameter ℓ. (NR —, ANN …) ($H_w = 20 \times 10^{-9}$, $w_b = 0{\cdot}32$, $I_s = 20 \times 10^{-10}$, $S_c = 8 \times 10^{-7}$).

frequencies can be calculated at once and retrieved as an output matrix without any convergence problems. In contrast, in the standard root finding technique, manual intervention may be necessary, since the algorithm may diverge and each root is calculated one by one for different frequencies and physical parameters. The total time required for an operator of the computer would then be much higher in the standard case.

4. INVESTIGATION OF THE EFFECT OF PHYSICAL PARAMETERS ON THE NATURAL FREQUENCIES

In this section, the effects of physical parameters on the natural frequencies are shown graphically. The results of the Newton–Raphson method are also plotted to make a comparison of the results of both methods. In Figures 4–8, the continuous lines represent the results of the Newton–Raphson method, whereas the dotted lines represent those of the ANN algorithm. A good match is observed between the methods.

In Figure 4, it is seen that the natural frequency decreases with increasing span length (ℓ). This variation becomes more pronounced in higher modes. Accordingly, the longer the span length of the bridge, the higher will be the vibration period.

In Figure 5, variation of the natural frequency with the dimensionless parameter H_w is shown. This parameter is directly proportional to the cable tension and inversely proportional the modulus of elasticity of the stiffening structure. Therefore, as the initial cable tension increases (or the modulus of elasticity of the stiffening structure decreases), the natural frequency decreases.

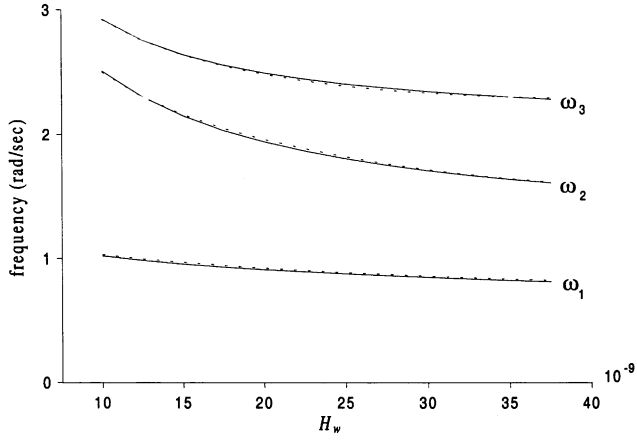

Figure 5. Variation of natural frequency with the dimensionless parameter H_w. (NR —, ANN ...) ($\ell = 4{\cdot}5$, $w_b = 0{\cdot}32$, $I_s = 16 \times 10^{-10}$, $S_c = 10 \times 10^{-7}$).

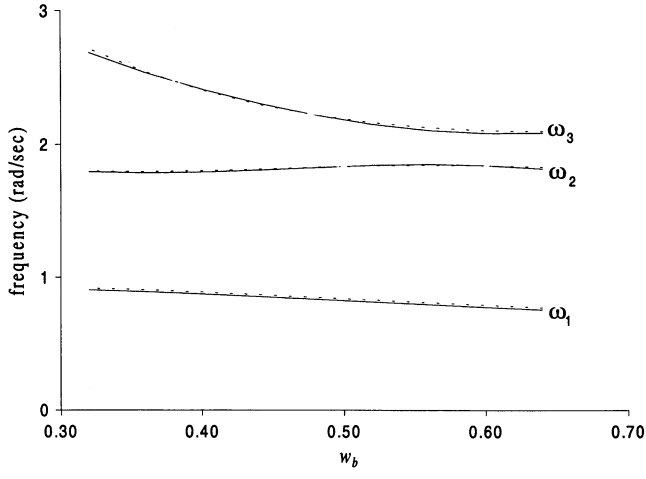

Figure 6. Variation of natural frequency with the dimensionless parameter w_b. (NR —, ANN ...) ($\ell = 4{\cdot}0$, $H_w = 20 \times 10^{-9}$, $I_s = 10 \times 10^{-10}$, $S_c = 7 \times 10^{-7}$).

In Figure 6, variation of the natural frequency with the dimensionless parameter w_b is shown. This parameter represents the dead weight of the bridge. The graphs indicate that increasing dead weight decreases the natural frequency in the first and third modes but have a very slight effect in the second mode. Thus, it can be concluded that the natural frequency is inversely proportional to the dead weight.

In Figure 7, variation of the natural frequency with the moment of inertia of the bridge cross-section is shown. It is observed that increasing moment of inertia increases the natural frequency. This is more pronounced in higher modes.

Figure 8 shows the variation of the natural frequency with the dimensionless parameter S_c. This parameter is directly proportional to the cables' modulus of elasticity and cross-sectional area and inversely proportional to the modulus of elasticity of the stiffening structure and virtual length. There is a very slight increase in the first and third modes whereas the increase in the second mode is apparent. It may not be appropriate to make

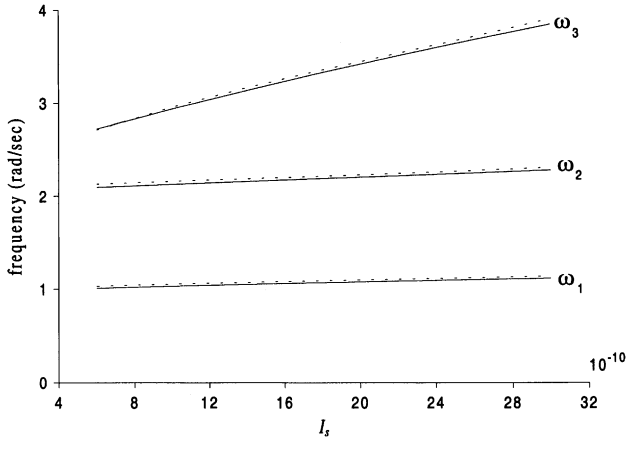

Figure 7. Variation of natural frequency with the dimensionless parameter I_s. (NR —, ANN ...) ($\ell = 3{\cdot}5$, $H_w = 17{\cdot}5 \times 10^{-9}$, $w_b = 0{\cdot}40$, $S_c = 10 \times 10^{-7}$).

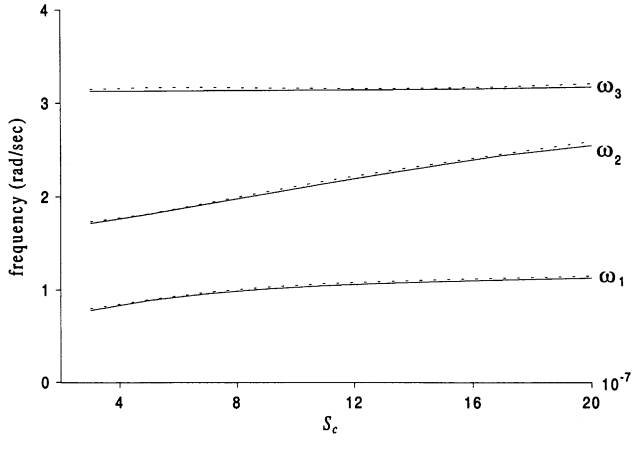

Figure 8. Variation of natural frequency with the dimensionless parameter S_c. (NR —, ANN ...) ($\ell = 3{\cdot}5$, $H_w = 20 \times 10^{-9}$, $w_b = 0{\cdot}40$, $I_s = 16 \times 10^{-10}$).

a generalization, yet one can conclude that the cables' modulus of elasticity and the cross-sectional area have an increasing effect on the natural frequency of the bridge.

5. CONCLUDING REMARKS

The calculation of the natural frequencies of suspension bridges and the parameters affecting the frequencies are studied. The exact values of the frequencies are calculated by the Newton–Raphson method. For each group of parameters, numerical analysis should be repeated, a lengthy process which requires the convergence of iterations. When the initial guesses are not close enough, the algorithm may diverge also. The method of ANN is used alternatively to compute the natural frequencies quickly and with small errors. Key values obtained by using the conventional analysis are used in training an ANN algorithm. After training, the algorithm yielded results with considerably low errors.

Then, the effects of physical parameters on the natural frequencies of suspension bridges are investigated using ANN. It is observed that the most effective parameters are the span length and the initial cable tension. The longer the span and the more the cable tension and the dead weight, the lower is the natural frequency. On the other hand, increasing moment of inertia, and the cables' modulus of elasticity and cross-sectional area slightly increases the natural frequencies.

REFERENCES

1. P. G. Buckland 1979 *American Society of Civil Engineers Journal of Structural Engineering* **105**, 859–874. Suspension bridge vibrations: computed and measured.
2. F. Van Der Woude 1982 *American Society of Civil Engineers Journal of Structural Engineering* **108**, 1815–1830. Natural oscillations of suspension bridges.
3. H. H. West, J. E. Suhoski and L. F. Geschwindner 1984 *American Society of Civil Engineers Journal of Structural Engineering* **110**, 2471–2486. Natural frequencies and modes of suspension bridges.
4. T. Kumarasena, R. H. Scanlan and G. R. Morris 1989 *American Society of Civil Engineers Journal of Structural Engineering* **115**, 2313–2328. Deer Isle Bridge: field and computed vibrations.
5. D. Bryja and P. Sniady 1988 *Journal of Sound and Vibration* **125**, 379–387. Random vibration of a suspension bridge due to highway traffic.
6. D. B. Steinman 1959 *Journal of Franklin Institute* **268**, 148–174. Modes and natural frequencies of suspension bridge oscillations.
7. A. M. Abdel-Ghaffar 1980 *American Society of Civil Engineers Journal of Structural Engineering* **106**, 2053–2075. Vertical vibration analysis of suspension bridges.
8. B. Karlik, E. Özkaya, S. Aydin and M. Pakdemİrlİ 1998 *Computers and Structures* **69**, 339–347. Vibrations of a beam–mass systems using artificial neural networks.
9. K. M. Abdalla and G. E. Stavroulakis 1995 *Microcomputing and Civil Engineering* **10**, 77–87. A backpropagation neural network model for semi-rigid steel connections.
10. L. Berke and P. Hajela 1992 *Structural Optimization* **4**, 90–98. Applications of artificial neural nets in structural mechanics.
11. H. A. Özyiğİt, B. Karlik and H. R. Öz 2001 *International Journal of Applied Mechanics and Engineering* **6**, 613–626. Active suspension control for vehicles and numerical calculations by using artificial neural networks.
12. E. Özkaya and M. Pakdemİrlİ 1999 *Journal of Sound and Vibration* **221**, 491–503. Non-linear vibrations of a beam-mass system with both ends clamped.
13. A. M. Abdel-Ghaffar and L. I. Rubin 1983 *American Society of Civil Engineers Journal of Engineering Mechanics* **109**, 313–329. Nonlinear free vibrations of suspension bridges: theory.